LETTER

A prevalence of dynamo–generated magnetic fields in the cores of intermediate–mass stars

Dennis Stello[1,2], Matteo Cantiello[3], Jim Fuller[3,4], Daniel Huber[1,2,5], Rafael A. García[6], Timothy R. Bedding[1,2], Lars Bildsten[3,7] & Victor Silva Aguirre[2]

Magnetic fields play a part in almost all stages of stellar evolution[1]. Most low-mass stars, including the Sun, show surface fields that are generated by dynamo processes in their convective envelopes[2,3]. Intermediate-mass stars do not have deep convective envelopes[4], although 10 per cent exhibit strong surface fields that are presumed to be residuals from the star formation process[5]. These stars do have convective cores that might produce internal magnetic fields[6], and these fields might survive into later stages of stellar evolution, but information has been limited by our inability to measure the fields below the stellar surface[7]. Here we report the strength of dipolar oscillation modes for a sample of 3,600 red giant stars. About 20 per cent of our sample show mode suppression, by strong magnetic fields in the cores[8], but this fraction is a strong function of mass. Strong core fields occur only in red giants heavier than 1.1 solar masses, and the occurrence rate is at least 50 per cent for intermediate-mass stars (1.6–2.0 solar masses), indicating that powerful dynamos were very common in the previously convective cores of these stars.

Red giants are formed when a low- or intermediate-mass star has finished burning the hydrogen in its core. This leaves an inert helium core surrounded by a thin hydrogen-burning shell and a very thick outer convective envelope. Like the Sun, red giants oscillate in a broad comb-like frequency spectrum of radial and non-radial acoustic modes that are excited by the turbulent surface convection[9]. The observed power spectrum has a roughly Gaussian envelope whose central frequency, ν_{max}, decreases as a star expands during the red giant phase[10]. The comb structure of the spectrum arises from a series of overtone modes separated by the so-called large frequency separation, $\Delta\nu$. One of these overtone sequences is seen for each spherical degree, ℓ. For observations of unresolved distant stars, geometric cancellation prevents the detection of modes with $\ell > 3$. Their spectra are characterized by a pattern of radial ($\ell = 0$) and quadrupolar ($\ell = 2$) modes that form close pairs, interspersed with dipolar ($\ell = 1$) modes located roughly halfway between successive radial-quadrupolar pairs. The octupolar modes ($\ell = 3$) are weak or undetectable. The dipolar modes have turned out to be particularly useful probes of internal structure[11]. They have been used to distinguish between hydrogen-shell and helium-core burning stars[12–14] and to measure radial differential rotation[15,16]. This is because each acoustic non-radial mode in the envelope couples to multiple gravity modes in the core, forming several observable mixed modes with frequencies in the vicinity of the acoustic mode[15]. This coupling is strongest for dipole modes, making them the most useful probes of the core[17].

Figure 1 shows the oscillation power spectra of red giants at three different evolutionary stages observed by NASA's Kepler mission. For 'normal' stars (upper panels in Fig. 1), the dipolar modes (red peaks) have
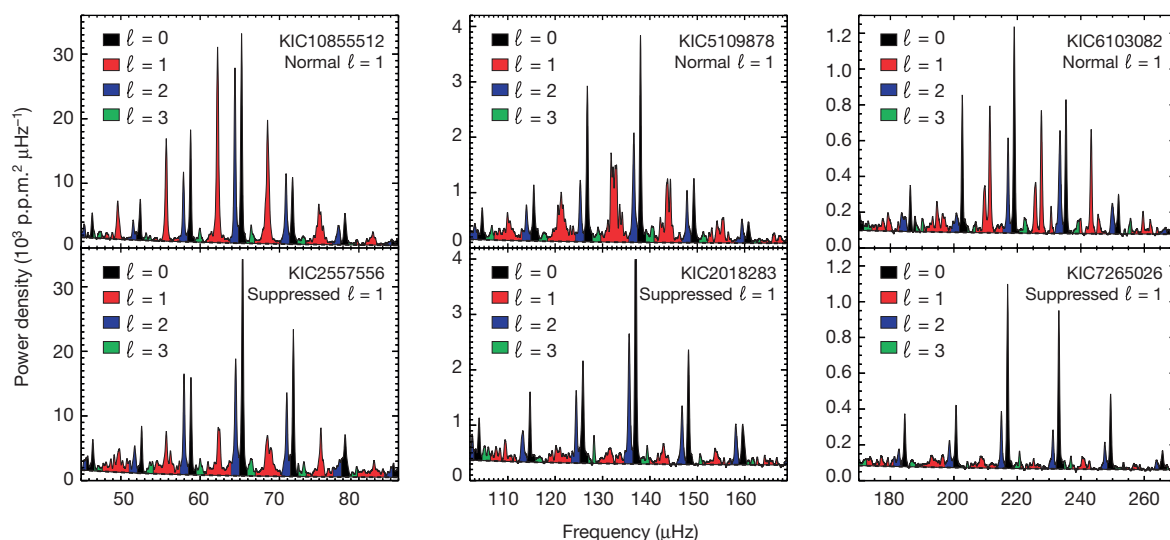
Figure 1 | Oscillation spectra of six red giants observed with Kepler. The stars are grouped into three pairs, each representing a different evolution stage ranging from the most evolved (lowest ν_{max}) on the left to the least evolved (highest ν_{max}) to the right. The coloured regions mark the power density dominated by modes of different degree $\ell = 0$–3. For clarity the spectra are smoothed by $0.03\Delta\nu$, which for the most evolved stars tends to create a single peak at each acoustic resonance, although each peak comprises multiple closely spaced mixed modes (red peaks in the left and centre panels). The slightly downward-sloping horizontal dashed line indicates the noise level.

[1]Sydney Institute for Astronomy (SIfA), School of Physics, University of Sydney, Sydney, New South Wales 2006, Australia. [2]Stellar Astrophysics Centre, Department of Physics and Astronomy, Aarhus University, Ny Munkegade 120, DK-8000 Aarhus C, Denmark. [3]Kavli Institute for Theoretical Physics, University of California, Santa Barbara, California 93106, USA. [4]TAPIR, Walter Burke Institute for Theoretical Physics, Mailcode 350-17, California Institute of Technology, Pasadena, California 91125, USA. [5]SETI Institute, 189 Bernardo Avenue, Mountain View, California 94043, USA. [6]Laboratoire AIM, CEA/DSM—CNRS—Université Paris Diderot—IRFU/SAp Centre de Saclay, 91191 Gif-sur-Yvette Cedex, France. [7]Department of Physics, University of California, Santa Barbara, California 93106, USA.
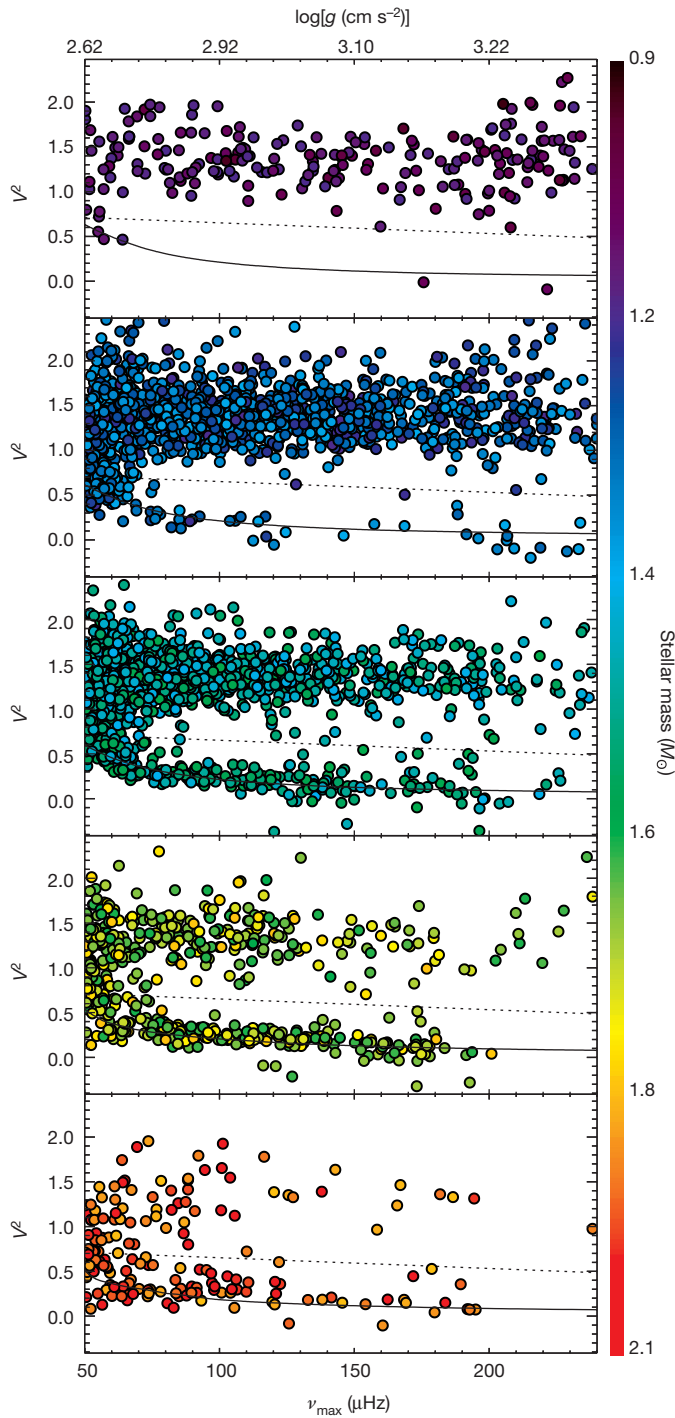
Figure 2 | Visibility of dipolar modes for red giants observed with Kepler. The abscissa shows the central frequency of each oscillation, which correlates closely with surface gravity (shown on the top axis). Stars evolve from right to left in the diagram, corresponding roughly to the beginning of the red giant phase to the red giant luminosity bump[27]. Stellar mass[13] (see colour scale on the right) has a formal 1σ uncertainty of 10% (ref. 28). The solid black line shows the theoretical predicted dipole-mode suppression[8] for $1.1M_\odot$, $1.3M_\odot$, $1.5M_\odot$, $1.7M_\odot$ and $1.9M_\odot$ (top to bottom panels) and a radial-mode lifetime of 20 days[29]. The fiducial dashed line separates normal and dipole-suppressed stars.

similar power to the radial modes (black peaks). However, at each stage of evolution we also find stars with greatly suppressed dipolar modes (lower panels in Fig. 1). Suppressed dipolar modes have been reported in a few dozen red giant stars[18,19], with an occurrence rate of about 20%.
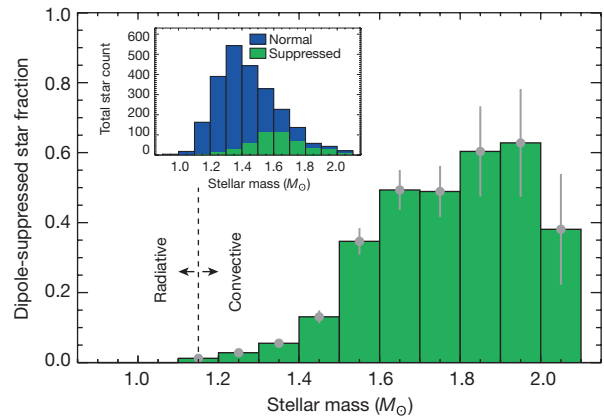
Figure 3 | Observed fraction of stars with suppressed dipolar modes. The abscissa is the stellar mass (in multiples of solar mass, $M_\odot$). Dipole-suppressed stars are defined as those that fall below the dashed line in Fig. 2. Only stars with $\nu_{max} > 70\,\mu$Hz are counted, to make the distinction between normal and suppressed unambiguous. The 1σ uncertainty in the fractions (grey vertical error bars) are based on Poisson statistics of the star counts (blue and green bars in the inset). The vertical dotted line separates stars for which hydrogen-core burning took place in either a radiative or convective environment for solar metallicity[4].

The cause of this phenomenon has been puzzling until recent theoretical work[8], which showed that the suppression can be explained if waves entering the stellar core are prevented from returning to the envelope. This occurs for dipolar modes if there are strong magnetic fields in the core, giving rise to a "magnetic greenhouse effect"[8].

We measured the amount of suppression by comparing the integrated power of the dipolar and radial modes (the dipole mode visibility, V^2), averaged over the four orders centred on ν_{max} (see Methods for details). While the normal stars show dipole mode visibilities of $V^2 \approx 1.5$, independently of ν_{max}, the stars with suppressed modes have $V^2 \approx 0.5$ for $\nu_{max} \approx 70\,\mu$Hz and down to almost zero for the least-evolved red giants oscillating above $200\,\mu$Hz (Fig. 1).

In Fig. 2 we show the dipole mode visibility for about 3,600 red giants observed over the first 37 months of the Kepler mission (see Methods). Our analysis is restricted to a sample of stars with ν_{max} larger than $50\,\mu$Hz and masses below $2.1M_\odot$ (where $M_\odot$ is the mass of the Sun), which, assuming no observational uncertainties, is expected to include only red giants that have not started burning helium in their cores[13]. We cross-matched our sample with those of known helium-burning stars[13,14], which allowed us to identify and remove a small fraction of evolved stars burning helium that, owing to measurement uncertainty, had entered our sample (2% of our sample, almost all with $\nu_{max} < 70\,\mu$Hz).

The stars in Fig. 2 form two distinct branches that gradually merge as the stars evolve leftwards towards lower ν_{max}. Most stars fall on the 'normal' upper branch of $V^2 \approx 1.5$, in agreement with previous results[18]. The lower branch, with suppressed dipole modes, agrees remarkably well with theoretical predictions (black curve). This prediction assumes that all the wave energy leaking into the stellar core is trapped by a magnetic greenhouse effect caused by strong internal magnetic fields[8]. The decrease of the suppression towards lower ν_{max} is a consequence of the weaker coupling between acoustic waves in the envelope and gravity waves in the core[8]. With this large sample we have been able to separate the stars in Fig. 2 into five different mass intervals, from $0.9M_\odot$ to $2.1M_\odot$. It is striking how strongly the relative population on the lower branch (stars with suppressed dipole modes) depends on mass.

We quantify the mass dependence in Fig. 3 by showing the relative number of dipole-suppressed stars (those below the dashed line in Fig. 2) in narrow mass intervals. We see no suppression in red giants below $1.1M_\odot$, which coincides with the mass below which they did not have convective cores during the core-hydrogen-burning phase[4].
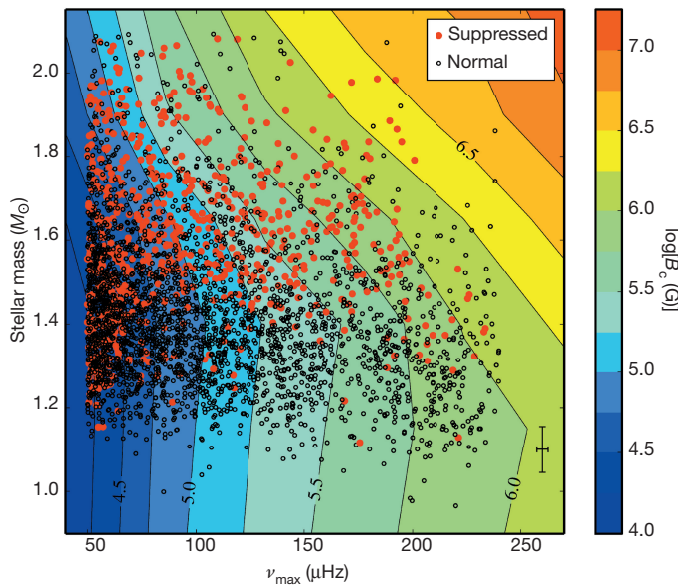
Figure 4 | Critical magnetic field strength required to suppress dipole mode oscillations. The abscissa is the observed central frequency of the oscillations. The ordinate is the inferred asteroseismic mass. The coloured contours indicate the minimum magnetic field at the hydrogen shell required for mode suppression (the critical field, B_c). Filled red circles mark stars with observed suppressed modes, and open circles mark normal (non-suppressed) stars. The cross shows a typical 1σ error bar for the data. The uncertainty in B_c due to uncertainty in mass is negligible for stars below $1.4M_\odot$ and is below 25% for the more massive stars.

The onset of magnetic suppression above this threshold suggests that at least some of those stars had convectively driven magnetic dynamos in their cores during the core-hydrogen-burning (main-sequence) phase. This is supported by three-dimensional hydrodynamical modelling of these stars[6]. Red giants no longer contain convective cores, leading us to conclude that the strong magnetic fields in suppressed oscillators are the remnants of the fields produced by core dynamos during the main sequence.

Figure 3 shows that the incidence of magnetic suppression increases with mass, with red giants above $1.6M_\odot$ showing a remarkable suppression rate of 50% to 60%. These have evolved from main-sequence A-type stars, among which only up to about 10% are observed to have strong fields at their surfaces[5]. We conclude that these magnetic A-type stars represent only the tip of the iceberg, and that a much larger fraction of A-type stars have strong magnetic fields hidden in their cores.

In Fig. 4 we show the observed ν_{max} and inferred mass of all the stars superimposed on a contour plot of minimum magnetic field strengths required for mode suppression[8]. For stars with suppressed modes (filled red circles), the underlying colour provides a lower bound to the field strength at the hydrogen-burning shell. For stars without suppressed modes (open black circles), the underlying colour represents an upper limit to the field at the hydrogen-burning shell; above or below the shell the field could potentially be larger. Hence, normal and dipole-suppressed stars that fall in the same regions of Fig. 4 may have core field strengths that are only slightly different. However, we expect that the dipole-suppressed stars on average exhibit stronger core fields than their normal counter parts.

Considering again the low-mass stars ($<1.1M_\odot$), of which none show suppression, we see from Fig. 4 that radial magnetic fields above about 100 kG are not present at the hydrogen-burning shell when the stars are just below the red giant luminosity bump ($\nu_{max} \approx 70$–$100\,\mu\text{Hz}$). Assuming magnetic flux conservation from the main-sequence phase, this suggests that radial fields above approximately 5 kG do not exist within the cores of Sun-like stars[8]. Large-scale fields in the solar interiors have been suggested to explain the properties of the tachocline[20]. However, our results do not rule out strong horizontal fields near the

radiative–convective boundary because those fields would be outside the core and could not cause mode suppression when the star evolves into a red giant.

Turning to higher masses we see that, for a given ν_{max}, stars above $1.4M_\odot$ require increasingly strong magnetic fields to suppress their dipolar modes. From Fig. 4, there is no clear upper limit to the field strengths present in red giant cores, given that dipole-suppressed stars are common even when field strengths $B > 1$ MG are required for suppression. However, the hint of a decline in the occurrence of dipole-suppressed stars above $2M_\odot$ seen in Fig. 3 suggests there may be a mass above which dynamo-generated magnetic fields are less likely to cause oscillation mode suppression in intermediate-mass stars.

The high occurrence rate of dipole mode suppression demonstrates that internal magnetic fields, generated by a convective core dynamo during the main sequence, can persist through the red giant phase. This indicates that these dynamo-generated fields are frequently able to settle into long-lived stable configurations[21,22]. The occurrence rate of suppressed dipole modes in intermediate-mass red giants is much higher than the occurrence rate of strong fields at the surfaces of the main-sequence A-type stars from which they evolved. These surface fields are thought to be a relic of the star's formation process[21,23]. We conclude that fields generated during convective hydrogen-core burning are able to settle into stable equilibrium configurations much more often (more than 50% of the time) than fields generated or inherited during star formation (less than 10% of the time).

Our results show that main-sequence stars with no observable magnetic field at the surface can still harbour strong fields in the core that survive into the red giant phase. The presence of internal magnetic fields might play an important part in angular momentum transport and potentially influence internal mixing processes. Fields too weak to suppress dipolar oscillation modes may exist in normal red giants, but these fields may nevertheless transport enough angular momentum to help explain the measured rotation rates of red giant cores[16,24]. The presence of strong internal magnetic fields might help to explain the extra internal mixing observed in red giant branch stars and asymptotic giant branch stars[25]. Interestingly, the magnetic field strength necessary for magnetic buoyancy mixing[26] is similar to the field strength required for dipole mode suppression[8].

After some time, intermediate-mass red giants also start burning helium in their cores. Suppressed dipolar modes in those so-called red clump stars will reveal whether the fields survive until helium-core burning, and whether they can account for magnetic fields observed in stellar remnants such as white dwarfs. Like intermediate-mass stars, more massive stars ($>10M_\odot$) also undergo convective hydrogen-core burning that generates a magnetic dynamo, and which may produce the magnetic fields observed in many neutron stars.

Online Content Methods, along with any additional Extended Data display items and Source Data, are available in the online version of the paper; references unique to these sections appear only in the online paper.

1. Landstreet, J. D. Magnetic fields at the surfaces of stars. *Astron. Astrophys. Rev.* **4,** 35–77 (1992).
2. Parker, E. N. Hydromagnetic dynamo models. *Astrophys. J.* **122,** 293–314 (1955).
3. Donati, J.-F. & Landstreet, J. Magnetic fields of nondegenerate stars. *Annu. Rev. Astron. Astrophys.* **47,** 333–370 (2009).
4. Kippenhahn, R. & Weigert, A. *Stellar Structure and Evolution* (Springer, 1990).
5. Power, J., Wade, G. A., Aurière, M., Silvester, J. & Hanes, D. Properties of a volume-limited sample of Ap-stars. *Contrib. Astron. Observ. Skalnate Pleso* **38,** 443–444 (2008).
6. Brun, A. S., Browning, M. K. & Toomre, J. Simulations of core convection in rotating A-type stars: magnetic dynamo action. *Astrophys. J.* **629,** 461–481 (2005).
7. Aurière, M. *et al.* The magnetic fields at the surface of active single G-K giants. *Astron. Astrophys.* **574,** A90 (2015).
8. Fuller, J., Cantiello, M., Stello, D., Garcia, R. A. & Bildsten, L. Strong internal magnetic fields explain suppressed oscillation modes in red giant stars. *Science* **350,** 423–426 (2015).

9. De Ridder, J. D. *et al.* Non-radial oscillation modes with long lifetimes in giant stars. *Nature* **459,** 398–400 (2009).
10. Stello, D., Bruntt, H., Preston, H. & Buzasi, D. Oscillating K giants with the *WIRE* satellite: determination of their asteroseismic masses. *Astrophys. J.* **674,** L53–L56 (2008).
11. García, R. A. & Stello, D. in *Extraterrestrial Seismology* (eds Tong, V. C. H. & García, R. A.) Ch. 11 (Cambridge Univ. Press, 2015).
12. Bedding, T. R. *et al.* Gravity modes as a way to distinguish between hydrogen- and helium-burning red giant stars. *Nature* **471,** 608–611 (2011).
13. Stello, D. *et al.* Asteroseismic classification of stellar populations among 13,000 red giants observed by Kepler. *Astrophys. J.* **765,** L41 (2013).
14. Mosser, B. *et al.* Mixed modes in red giants: a window on stellar evolution. *Astron. Astrophys.* **572,** L5 (2014).
15. Beck, P. G. *et al.* Kepler detected gravity-mode period spacings in a red giant star. *Science* **332,** 205 (2011).
16. Mosser, B. *et al.* Spin down of the core rotation in red giants. *Astron. Astrophys.* **548,** A10 (2012).
17. Dupret, M.-A. *et al.* Theoretical amplitudes and lifetimes of non-radial solar-like oscillations in red giants. *Astron. Astrophys.* **506,** 57–67 (2009).
18. Mosser, B. *et al.* Characterization of the power excess of solar-like oscillations in red giants with Kepler. *Astron. Astrophys.* **537,** A30 (2012).
19. García, R. A. *et al.* Study of KIC 8561221 observed by Kepler: an early red giant showing depressed dipolar modes. *Astron. Astrophys.* **563,** A84 (2014).
20. Gough, D. O. & McIntyre, M. E. Inevitability of a magnetic field in the Sun's radiative interior. *Nature* **394,** 755–757 (1998).
21. Braithwaite, J. & Spruit, H. C. A fossil origin for the magnetic field in A stars and white dwarfs. *Nature* **431,** 819–821 (2004).
22. Duez, V., Braithwaite, J. & Mathis, S. On the stability of non-force-free magnetic equilibria in stars. *Astrophys. J.* **724,** L34–L38 (2010).
23. Moss, D. On the magnetic flux distribution in magnetic CP stars. *Mon. Not. R. Astron. Soc.* **226,** 297–307 (1987).
24. Cantiello, M., Mankovich, C., Bildsten, L., Christensen-Dalsgaard, J. & Paxton, B. Angular momentum transport within evolved low-mass stars. *Astrophys. J.* **788,** 93 (2014).
25. Busso, M., Wasserburg, G. J., Nollett, K. M. & Calandra, A. Can extra mixing in RGB and AGB stars be attributed to magnetic mechanisms? *Astrophys. J.* **671,** 802–810 (2007).
26. Nucci, M. C. & Busso, M. Magnetohydrodynamics and deep mixing in evolved stars. I. Two- and three-dimensional analytical models for the asymptotic giant branch. *Astrophys. J.* **787,** 141 (2014).
27. Salaris, M. & Cassisi, S. *Evolution of Stars and Stellar Populations* (John Wiley & Sons, 2005).
28. Miglio, A. *et al.* Asteroseismology of old open clusters with Kepler: direct estimate of the integrated red giant branch mass-loss in NGC 6791 and 6819. *Mon. Not. R. Astron. Soc.* **419,** 2077–2088 (2012).
29. Corsaro, E., Ridder, J. D. & Garcia, R. A. Bayesian peak bagging analysis of 19 low-mass low-luminosity red giants observed with Kepler. *Astron. Astrophys.* **579,** A83 (2015).

Author Contributions D.S. measured and interpreted mode visibilities; M.C. and J.F. calculated and interpreted theoretical models; D.H. and D.S. calculated power spectra and measured large frequency separations; R.A.G., T.R.B., L.B. and V.S.A. contributed to the discussion of the results. All authors commented on the manuscript.

Author Information Reprints and permissions information is available at www.nature.com/reprints. The authors declare no competing financial interests. Readers are welcome to comment on the online version of the paper. Correspondence and requests for materials should be addressed to D.S. (stello@physics.usyd.edu.au).

METHODS

Dipole mode visibilities. For each star in our sample we derived the frequency power spectrum as the Fourier transform of the Kepler light curve (up to observing quarter 14) and adopted the values of $\Delta\nu$, ν_{max} and mass from previous work[13]. To correct the spectrum for the background noise, we measured and subtracted a linear slope anchored on the median power on either side of the central power excess, defined by the frequency ranges $0.75(\nu_{max} - 2\Delta\nu)$ to $(\nu_{max} - 2\Delta\nu)$ and $(\nu_{max} + 2\Delta\nu)$ to $1.25(\nu_{max} + 2\Delta\nu)$. We then selected a $4\Delta\nu$-wide range of the spectrum centred on ν_{max}. The location of each mode was found by first folding this central part of the spectrum using $\Delta\nu$ as the folding frequency such that modes of the same spherical degree each formed a single peak. The folded spectrum was smoothed by a Gaussian filter with a width of $0.1\Delta\nu$. We finally correlated the folded spectrum with a model spectrum comprised of three Lorenzian profiles, one for each degree $\ell = 0$, 1 and 2, with relative heights of 1.0, 0.5 and 0.8, and widths of 5%, 10% and 5% of $\Delta\nu$, respectively. The centres of each Lorenzian profile were fixed relative to one another such that the one representing the $\ell = 2$ modes was $0.12\Delta\nu$ to the left (lower frequency) of the $\ell = 0$ profile, and the $\ell = 1$ profile was $0.52\Delta\nu$ to the right (higher frequency)[30]. The shift between the model and the observed folded spectrum that gave the largest correlations provided the location of each mode. The regions of the power spectrum associated with each spherical degree were set to be $0.16\Delta\nu$, $0.53\Delta\nu$ and $0.16\Delta\nu$ wide for $\ell = 0$–2, respectively, with the regions located according to the mode location found by the correlation with the model spectrum. The remaining region was associated with $\ell = 3$ modes (Fig. 1). The dipole-mode visibility was derived as the integrated power of the dipole modes relative to that of the radial modes, following the approach by previous studies[18].

Code availability. We used the commercially available IDL routine *lnp_test* to derive the Fourier spectra of the Kepler light curves. To derive the mode visibilities we used built-in IDL routines and subroutines written by others, which are therefore not made publicly available. For the stellar evolution calculations we used MESA (publicly available at http://mesa.sourceforge.net/).

30. Huber, D. *et al.* Asteroseismology of red giants from the first four months of Kepler data: global oscillation parameters for 800 stars. *Astrophys. J.* **723,** 1607–1617 (2010).